

Array Mode Characteristics of Channeled-Substrate - Planar Phased Laser Arrays

(CSP 레이저 어레이의 결합모드 특성)

제롬 버틀러*, 吳煥述**

(J. K Butler and Hwan Sool Oh)

要 約

CSP 레이저들의 線形어레이들의 모오드에 대한 발전과정과 利得특성을 나타내었다. 어레이모우드들의 利得값들은 배열이 인접한 요소들의 場을 이용하여 계산된 복소결합계수들로 결정된다. 계산결과는 거의 실수값인 場을 갖는 index guided lasers에 대하여 最高次어레이모우드가 쉽게 발진함을 보였다. Far field radiation pattern에서 단지 하나의 단일로브만 이루어지는 基本모우드는 모든 어레이모우드 중 가장 낮은 모우드利得을 가졌다. 最高次모우드와 基本모우드 사이에서 10cm^{-1} 보다 적은 모우드利得차이를 이뤘고 이것은 약20%의 光拘束因子에 대해서, 利得차는 근사적으로 50cm^{-1} 의 활성층 利得에 해당되었다.

Abstract

The lasing wavelengths and gain characteristics of the array modes of channel-substrate-planar (CSP) lasers are presented. The gain values of array modes are determined from the complex coupling coefficients calculated using the fields of neighboring elements of the array. The computations show that for index guided lasers which have fields that are almost real valued, or have only slight phase curvature, the highest order array mode will have preferred oscillation. The inphase or fundamental mode, which produces only one major lobe in the far-field radiation pattern, will have the lowest modal gain of all array modes. Some of the devices discussed have modal gain differences of less than 10 cm^{-1} between the highest and fundamental modes. For optical field confinement factors of about 20%, this gain difference corresponds to active layer gains of approximately 50 cm^{-1} .

Introduction

The development of injection laser technology has progressed over the past several years to a level of sophistication so that linear arrays of individual laser elements can be fabricated

on a single wafer. [1-5] Laser arrays are becoming popular because many applications require large amounts of optical power which cannot be obtained from single contemporary lasers. Typically, the emission power level from an injection laser is related to the volume occupied by the lasing mode. Broad area device emits high power, but its optical mode stability is not good. These instabilities occur because of nonlinear interaction between the optical mode and the waveguide which is defined by both a real and imaginary part of the dielectric constant. [6,7]

*正會員, 남감리大學校 電氣工學科

(Southern Methodist University Dallas, Texas 75275, USA)

**正會員, 建國大學校 電子工學科

(Dept. of Elec. Eng., Kon-Kuk Univ.)

接受日字: 1986年 5月 2日

The analysis of injection laser phased arrays using coupled mode theory has been recently presented. [8-10] However, these earlier analyses have included only the effects of passive systems, i.e., gain and loss considerations of the array were not analyzed. However, a similar analyses using a different approach have been presented [11,12]. In this paper we discuss the results associated with the analysis of phased arrays when both the passive and active nature of the waveguide are included in the problem. In particular, in a passive structure the coupled-mode analysis gives only a splitting of the propagation constant which relates to the possible mode oscillation wavelengths. In an active structure, both the gain and refractive index distributions affect mode characteristics; the wavelength splitting and the gain splitting of the individual laser modes. The gain splitting is important because it determines individual array mode. In this paper we will address the array mode gain splitting from an analysis of the coupled-mode equations.

Array Element Characterization

A discussion of the coupled modes can be effected provided a detailed analysis of the optical field of the individual elements is fully characterized. To produce a noticeable degree of coupling it is necessary that each element be nearly identical as possible. First, we put into context the character of the individual elements. The single element will be described by a field distribution $\Psi^n(x, y, z)$ where the superscript pertains to the n-th device. If the individual lasers are separated by a distance s , then the array is uniformly spaced. The overall array aperture size is a multiple of the spacing. For example, for N elements, the aperture size is $N \times s$. On the other hand, if the elements are located at points $y = s_n$, then the aperture size is $s_1 - s_N$. Because the elements are identical, the fields satisfy the condition $\Psi^1(x, y + s_{1,2}) = \Psi^n(x, y + s_{n,2})$. The optical field of the m-th element satisfies the wave equation

$$\nabla^2 \Psi^m + k_0^2 k^m(x, y) \Psi^m = 0 \tag{1}$$

where the wave function is written as

$$\Psi^m(x, y, z) = u^m(x, y) v^m(y) \exp(-\gamma_m z) \tag{2}$$

where $u^m(x, y)$ describes the transverse (to the junction) profile while $v^m(y)$ governs the lateral mode profile. (The index m pertains to the m -th element.) The transverse field function $u^m(x, y)$ has a y -dependence which is due to layer thickness variations found in CSP lasers. The wave function $v^m(y)$ satisfies

$$\frac{d^2 v^m}{dy^2} + [\gamma_m^2 - \gamma_{0m}^2(y) + k_0^2 \Gamma^m(y) k_v^m(y)] v^m = 0 \tag{3}$$

where Γ_m is the complex optical confinement factor of the field to the active layer, and k_v^m is the perturbation of the active layer dielectric constant from its passive value. The quantity $\gamma_{0m}(y) = \alpha_e(y) + j k_0 n_e(y)$ where $\alpha_e(y)$ and $n_e(y)$ are the effective absorption coefficient and effective index of refraction in the lateral direction. (The index m is dropped from α_e and n_e expressions because we assume identical array elements.) For example, in Fig. 2 we show $\alpha_e(y)$ and $n_e(y)$ as a function of lateral position for two element types used for the fabrication of arrays. The basic structures with material parameters as given in table 1 are shown in Fig. 1. It should be noted that these structures exhibit index guiding along the lateral direction. The dielectric variation of the active layer for the single element m is

$$k_v^m(y) = 2n_2 \nabla n_2^m + j \frac{n_2 g^m(y)}{k_0} \tag{4}$$

where ∇n_2^m is given by the ad hoc relation [8].

$$\nabla n_2^m = \frac{R \nabla g^m}{k_0} \tag{5}$$

where the proportionality constant R is taken as -2. This equation simply ties the index change at a point in the active layer to the gain at that position using a linear relationship. Including both the effective complex propagation constant and the perturbation of the active layer dielectric constant from eq. (3) and eq. (4), the total dielectric variation (of the single element m) along y becomes

$$k^m(y) = |n_e^m(y)|^2 - \left[\frac{\alpha_e^m(y)}{k_0} + 2\Gamma^m(y) n_2 \nabla n_2^m \right] - j \left[\frac{2n_e^m \alpha_e^m(y)}{k_0} - \frac{\Gamma^m(y) n_2 g^m(y)}{k_0} \right] \tag{6}$$

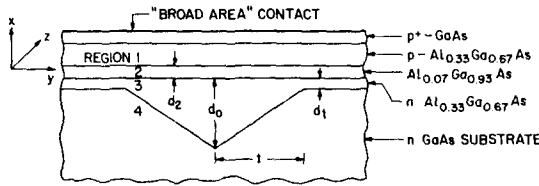


Fig. 1. The geometries of the CSP laser structures used for the calculations. The contact and thus the applied current is extended uniformly over all elements of the array.

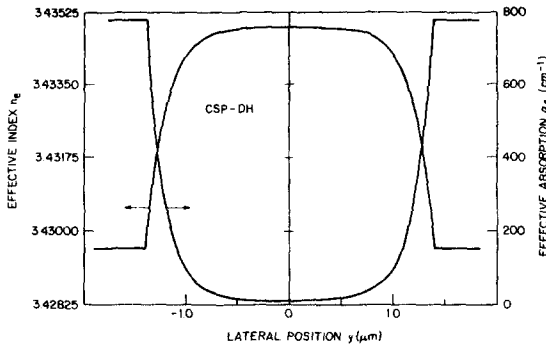


Fig. 2. The effective index and absorption coefficient profiles for the CSP element.

For devices with a uniform active layer such as in the CSP lasers, the active region gain $g^m(y)$ is independent of lateral position provided the stripe contact is much larger than the taper lengths of the cladding n-layer. Nevertheless, the variations of the two terms in the imaginary part of k^m are y dependent so that both the real and imaginary parts of the dielectric constant are y dependent.

Table 1. Optical Constants

Region	Refractive Index	Absorption
		Coefficient (cm ⁻¹)
1	3.41	10
2	3.62	--
3	3.62	10
4	3.64	5000

Array Formalism

To discuss the total array field it is necessary

to solve Maxwell's equations for the coupled lasers which we assume are identical. The electric field of the individual devices is composed of solutions of the wave equation discussed in the previous section. Assuming the fields are polarized along y as in Fig. 1, we have for the individual laser (m-th element)

$$E_{y,m} = u^m(x, y) v^m(y) \exp(-\gamma_m z) = e_{y,m} \exp(-\gamma_m z) \tag{7}$$

These modes are almost transverse electric field (TE) as initially described by Marcatilli. [13] The largest transverse magnetic field component $H_{x,m} = \frac{\gamma_m}{j\omega\mu_0 E_{y,m}}$ is polarized along x. The field in Eq. (7) represents a wave propagating in the positive z direction. The waves propagating in the negative z direction also satisfy Maxwell's equations. Solutions are similar to those of Eq. (7), but γ_m is replaced by $-\gamma_m$ and the magnetic field component reverses its direction. We denote the major transverse field components of backward wave as $E_{y,\bar{m}}$ and $H_{x,\bar{m}}$. The coupled-mode analysis of the array field is effected by writing the total field as a linear combination of fields of the individual lasers [14]:

$$\vec{E} = \sum_m A^m(z) \vec{E}_m \tag{8a}$$

$$\vec{H} = \sum_m A^m(z) \vec{H}_m \tag{8b}$$

Substituting Eq. (8) into the pair of Maxwell's curl equations gives

$$\sum_m A^m [\nabla_t \times \vec{H}_m - \gamma_m (\hat{z} \times \vec{H}_m)] + (\hat{z} \times \vec{H}_m) \frac{dA_m}{dz} - j\omega\epsilon_0 k A^m \vec{E}_m = 0 \tag{9a}$$

$$\sum_m A^m [\nabla_t \times \vec{E}_m - \gamma_m (\hat{z} \times \vec{E}_m)] + (\hat{z} \times \vec{E}_m) \frac{dA_m}{dz} + j\omega\mu_0 A_m \vec{H}_m = 0 \tag{9b}$$

where k is the array dielectric constant and ∇_t is the transverse vector operator. The two above equations can be simplified, using the field solutions for the single element in the absence of coupling, to:

$$\sum_m [A^m j\omega\epsilon_0 (k_m - k) \vec{E}_m + (\hat{z} \times \vec{H}_m) \frac{dA_m}{dz}] = 0 \tag{10a}$$

$$\sum_m (\hat{z} \times \vec{E}_m) \frac{dA_m}{dz} = 0 \tag{10b}$$

To reduce the z dependence in the field expressions which contain the complex propagation constant it is necessary to scalar multiply Eq. (10a) by \bar{E}_n^- and (10b) by \bar{H}_n^- the backward wave solutions. Upon integration, we obtain the following set of coupled equations

$$\frac{dA^n}{dz} = \frac{k_0^2}{2} \sum_m \frac{1}{\gamma_n} c_{nm} A^m \quad (11)$$

where the coupling coefficient c_{nm} is

$$c_{nm} = \frac{-2j\omega\epsilon_0\gamma_n}{k_0^2} \frac{\int \int (\mathbf{k} - \mathbf{k}_m) \bar{e}_n^- \cdot \bar{e}_m^- \exp[(\gamma_n - \gamma_m)z] dx dy}{\int \int \hat{z} \cdot [(\bar{e}_n^- \times \bar{h}_n^-) - (\bar{e}_m^- \times \bar{h}_m^-)] dx dy} \quad (12a)$$

$$c_{nm} = \frac{\int \int (\mathbf{k} - \mathbf{k}_m) (u^m u^n v^m v^n) dx dy}{\int \int (u^m u^n v^m v^n) dx dy} \quad (12b)$$

where $\bar{e}_n^- = \hat{y} u^n(x, y) v^n(y)$ and $\bar{h}_n^- = -\hat{x} \frac{\gamma_n}{j\omega\mu_0} v^n(x, y), v^m(y)$. If the array elements are identical, then $\gamma_n = \gamma_m$, and the above coupling coefficients simplify to

Since the dielectric constants and the field expressions are complex quantities, the resulting coupling coefficient is a complex number. The numerical values of c_{nm} will be discussed in a later section.

Array Modes

The array modes of a group of coupled lasers can be obtained by solving the set of simultaneous given by Eq. (11). First, we address the functional dependence of A^m with respect to z since this affects array mode solutions. Because A^m is a weakly varying function of z under weak coupling, it is convenient to put

$$A^m(z) = A_0^m \exp(-\delta_m z) \quad (13)$$

It is obvious that for zero coupling, $\delta_m = 0$. It is further important to note that if δ_m were element dependent, it would be impossible to establish the resonant condition simultaneously for each laser element. Consequently, an overall array mode would not exist [8]. Thus, array modes have δ_m as m independent so that

the subscript will be dropped. Substitution of Eq. (13) into Eq. (11) gives

$$\sum_m c_{nm} A_0^m + \frac{2\gamma\delta}{k_0^2} A_0^n = 0 \quad (14)$$

so that the above equation reduces to the well-known eigenvalue equation of the form

$$C_a = \mu a \quad (15)$$

where $\mu = \frac{-2\gamma\delta}{k_0^2}$ the eigenvalue, a is the corresponding eigenvector

$$a = \begin{bmatrix} A_0^1 \\ A_0^2 \\ A_0^3 \\ \vdots \\ A_0^N \end{bmatrix} \quad (16)$$

and the bidiagonal matrix C is

$$C = \begin{bmatrix} 0 & c_{12} & 0 & \cdots & 0 \\ c_{21} & 0 & c_{23} & \cdots & 0 \\ 0 & c_{32} & 0 & \cdots & 0 \\ \vdots & \vdots & \vdots & \ddots & \vdots \\ 0 & 0 & 0 & \cdots & 0 \end{bmatrix} \quad (17)$$

Because C is bidiagonal, a generalized second order difference equation for the eigenvalue problem can be written as

$$c_{n,n-1} A_0^{n-1} + c_{n,n+1} A_0^{n+1} = \mu A_0^n \quad (18)$$

(A fourth order difference equation results upon extension of C to a quadriagonal matrix. This occurs when a specific laser couples to 4 of its nearest neighbors.) Although Eq. (18) cannot be solved in closed form, it can be greatly simplified once the array geometry is specified. For example, when the elements are uniformly spaced, all elements of the coupling matrix are identical, i.e., there is equal coupling to each nearest neighbor. Consequently, Eq. (18) becomes

$$A_0^{n-1} - \frac{\mu}{c} A_0^n + A_0^{n+1} = 0 \quad (19)$$

where $c = c_{nm} = c_r + j c_i$ is the coupling

coefficient. Now, by putting $A_0^n = Q \exp(jn\phi)$ where Q and ϕ are unknown constants. The resulting characteristic equation becomes

$$\exp(-j\phi) - \frac{\mu}{c} + \exp(j\phi) = 0 \quad (20)$$

which yields a solution for the eigenvalue

$$\mu = 2c \cos(\phi) \quad (21)$$

Since Eq. (19) is a second order difference equation, a second solution is $A_0^n = Q \exp(-jn\phi)$. To find the specific value of A_0^n we apply the boundary condition to the general solution, written as

$$A_0^n = Q_1 \cos(n\phi) + Q_2 \sin(n\phi) \quad (22)$$

which is a linear combination of the two exponential solutions. Since we are interested only in the A_0^n values lying in the range $1 < n < N$, we can place $A_0^0 = A_0^{N+1} = 0$. Substitution into Eq. (22) yields

$$(N+1)\phi = p\pi, \quad p = 1, 2, 3, \dots, N \quad (23)$$

The integer p now corresponds to the array modes; $p = 1$ is the fundamental, where as $p = N$ is the highest order one. The array excitations become

$$A_{0,p}^n = Q_2 \sin\left(\frac{np\pi}{N+1}\right) \quad (24a)$$

where as, the eigenvalues become

$$\mu_p = 2c \cos\left(\frac{p\pi}{N+1}\right) \quad (24b)$$

The constant θ_2 may be calculated from a normalization condition. The value of $\delta_p = \frac{k_0^2 \mu_p}{2\gamma}$ represents the split of the propagation constant from that of the single element value, γ . Hence, the array modes have

$$\gamma_p = \gamma \left[1 - c \frac{k_0^2}{\gamma^2} \cos\left(\frac{p\pi}{N+1}\right) \right] \quad (25)$$

The wavelength and gain coefficient of the p -th array mode are determined from the complex coupling coefficient and from the unperturbed

single element. The value $\gamma = \alpha + j\beta$ where $G = -2\alpha$ is the normalized modal gain coefficient of the single laser element. In contemporary laser structures, $\beta \gg \alpha$. Thus, Eq. (25) can be simplified

$$\gamma_p = \alpha + j\beta - \left(\frac{k_0}{n_e} \right) |c_l - ic_r| \cos\left(\frac{p\pi}{N+1}\right) \quad (26)$$

Here, $n_e = \frac{\beta}{k_0}$ is the mode effective index of refraction. For $c_r > 0$, the wavelength of the $p = 1$ mode is longer than that of a single element laser, while for $p = N$, the array mode wavelength is shorter than it. The mode oscillation wavelength and gain coefficient are

$$\frac{(\lambda_p - \lambda_0)}{\lambda_p} = \frac{-c_r}{n_e^2} \cos\left(\frac{p\pi}{N+1}\right) \quad (27a)$$

$$G_p = G + \left(\frac{2k_0 c_l}{n_e} \right) \cos\left(\frac{p\pi}{N+1}\right) \quad (27b)$$

Note that for $c_l > 0$, the fundamental mode ($p = 1$) is favored while for $c_l < 0$, the highest order mode ($p = N$) lases.

The complex propagation constant γ_p and array excitation function given by Eq. (24a) are sufficient to characterize the array radiation pattern $F_p(\theta)$ in the junction plane. The overall pattern in the lateral plane is the product of the element pattern $f(\theta)$ and the array pattern function. Thus, the exact nature of the element pattern which is the Fourier transform of its facet field, need not be known in order to compute the array pattern.

In simple diffraction theory where the amplitudes of all elements are identical, the far field intensity of a uniformly spaced array is

$$I(u) = \frac{\sin^2\left(\frac{Nsu}{2}\right)}{\sin^2\left(\frac{su}{2}\right)} \quad (28)$$

where $u = k_0 \sin \theta$. In the coupled mode theory developed here, the far field intensity pattern becomes

$$I_p(u) = \frac{\sin^2\left[\frac{s(N+1)u}{2} + \frac{p\pi}{2}\right]}{\left[\sin^2\left(\frac{su}{2}\right) - \sin^2\left(\frac{p\pi}{2(N+1)}\right)\right]^2} \quad (29)$$

For the case $N \gg 1$, the patterns of a uniformly spaced array with equal amplitudes differ from that of an array with coupled mode tapered amplitudes. Typically, arrays with tapered amplitudes produce far-field beamwidths which are larger than that for uniform amplitudes. Also, array pattern sidelobes are smaller for nonuniform tapers than for that of uniform tapers. A detailed discussion of the far-field patterns of the various array modes is given by D. Botez [15] and D.E. Ackley [16].

Coupling Coefficient

In this section we discuss the characteristics of the individual laser elements and how they couple to one another in the array environment. Because the CSP type structures have lateral waveguides that are strongly developed by both the real and imaginary parts of the dielectric constant, the optical fields will be complex. Consequently, the coupling coefficients as given by Eq. (12b) will be complex. The propagation constant of a single laser will, therefore, split into $\delta_p = \frac{-k^2 \mu_p}{2\gamma}$ of complex numbers that represent the propagation constants of the individual array modes. The imaginary part of the splitting affects the lasing frequency while the real part characterizes the array model gains.

From Fig. 2 we see that the CSP structures have effective indices such that the modes will be strongly index guided. Thus, the wave functions have very little phase variation in the lateral direction which means that the fields are almost real valued. The evanescent fields will have exponential decay which greatly affects the coupling coefficients. In fact, the magnitude of c will decay exponentially with respect to element spacing. To get a rough estimate of c , we assume that the lateral modes can be characterized by a simple three layer slab waveguide. As can be seen from the index variations of Fig. 2, this assumption is relatively good.

Figure 3 illustrates the calculated values of $c = c_r + jc_i$ as a function of laser separation, s . These calculations were made for a series of active layer thicknesses and material composi-

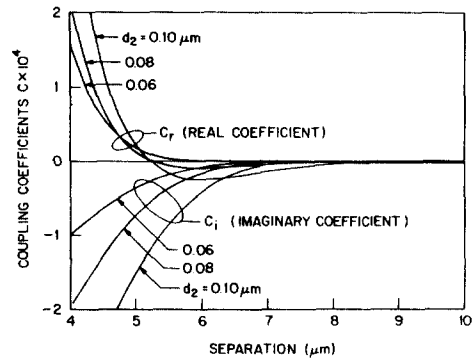


Fig. 3. The coupling coefficient $c = c_r + jc_i$ for CSP type phased-array structures as a function of element separation. The active layer thickness d_2 is a parameter and the active layer to substrate thickness d is $0.3 \mu m$.

tions as given in table 1. The gain coefficient of the active layer was adjusted so that the modal gain coefficient of a single element laser was 50 cm^{-1} , sufficient to offset end losses. As illustrated, when $s > 7 \mu m$, the coupling coefficient is very small. For the case $d_2 = 0.08 \mu m$, the effective index is illustrated in Fig. 2, but for different d_2 values, the effect on the lateral modes affects c in a profound way: as d_2 increases, the lateral modes become tightly bound, while for d_2 decreasing, the lateral modes become loosely bound. This is in part due to the sloping sides of the particular CSP design.

Consider now the gain coefficient of the array modes for $d_2 = 0.08 \mu m$ and $s = 5 \mu m$. The resulting coupling coefficients are $c_r = 0.2 \times 10^{-4}$ and $c_i = -0.8 \times 10^{-4}$. The wavelength splitting is

$$\frac{(\lambda_p - \lambda)}{\lambda_p} = -1.6 \times 10^{-6} \cos\left(\frac{p\pi}{N+1}\right) \quad (30)$$

and the gain splitting is

$$G_p - G = -3.5 \cos\left(\frac{p\pi}{N+1}\right) \text{ cm}^{-1} \quad (31)$$

The fundamental mode of a 10 element array, has $G_1 - G = -3.3 \text{ cm}^{-1}$ while the highest order mode has $G_{10} - G = +3.3 \text{ cm}^{-1}$.

Thus, the highest-order array mode will lase because it has the largest gain coefficient. This

means the gain of the active layer will be smaller for the highest order array mode than for the single laser operating without coupling. Correspondingly, the inversion level will be smaller than that of the isolated laser. From the coupling coefficient versus the element spacing, the main observation is the fundamental dependence of c and s ; that functional dependence is exponential, (ref. Fig. 3). This occurs because the field strength in a neighboring laser has an exponentially decaying fields.

Conclusion

In this paper we have presented an analysis of injection laser phased arrays using coupled mode theory. In the theoretical model it was necessary to introduce the backward wave solutions in order to reduce the z dependence in the expression of the coupling coefficient. The exclusion of z dependence in the coupling matrix simplifies the simultaneous differential equations governing the coupled modes.

The results of laser coupling to only nearest neighbors affords a simple solution to the splitting phenomena. The analysis can be extended to include coupling to all elements of the array. The coupling coefficients will be rather small when distances are larger than about 7 μm . Thus, the models using only nearest neighbor coupling appear to be rather accurate.

The calculation of the complex coupling coefficient is useful because the complex propagation constant of array modes can be determined. Using lossless waveguide materials, coupling coefficients relate only to the oscillation wavelengths. The model presented here allows for the computation of both array mode oscillation wavelengths and modal gains.

For uniformly spaced arrays, the array modal gains are distributed about the modal gain of the isolated laser element. When the imaginary part of the coupling coefficient c_i is negative, as is the case for the CSP laser structures presented here, the highest order array mode has the largest modal gain so that it will reach threshold before all the other array modes. On the other hand, the fundamental array mode will have the lowest gain when c_i is negative. Accordingly, it will

require the highest gain at threshold. Physically, the highest order mode has fields with differential phase shifts of 180° between neighboring elements. Consequently, the array mode will have a null value at midpoints between the individual lasers. Since the nulls occur in the high absorption region, losses are minimized. On the other hand, the fundamental mode will not have field nulls in the lossy regions and consequently, it will have the higher absorption losses.

References

- [1] D.E. Ackley, "Single longitudinal mode operation of high power multiple-stripe injection laser," *Appl. Phys. Lett.*, vol. 42, pp. 152-154, Jan. 1983.
- [2] D.R. Scifres, C. Lindstrom, R.D. Burnham, W. Streifer and T.L. Paoli, "Phase-locked (GaAl)As laser diode emitting 2.6w cw from a single mirror," *Electron. Lett.*, vol. 19, pp. 169-171, Mar. 1983.
- [3] D. Botez, and J.C. Connolly, "High-power phase-locked array of index-guided diode lasers," *Appl. Phys. Lett.*, vol. 43, pp. 1096-1098, Dec. 1983.
- [4] J.R. van der Ziel, R.A. Logan, and R.M. Mikulyak, "A closely space (50 μm) array of 16 individually addressable buried heterostructure GaAs lasers," *Appl. Phys. Lett.*, vol. 41, pp. 9-11, July 1, 1982.
- [5] F. Kappeler, H. Westermeier, R. Gessner, M. Druminski and K.H. Zschauer, "High cw power arrays of optically coupled (GaAl)As oxide stripe lasers with dc-to-light conversion efficiencies of up to 36%," Ninth IEEE International Semiconductor Laser Conference, Rio de Janeiro, Brazil, August 7-10, 1984.
- [6] W. Streifer, R.D. Burnham and D.R. Scifres, "An analytic study of (GaAl)As gain guided lasers at threshold," *IEEE J. Quantum Electron.*, vol. QE-18, pp. 856-864, May 1982.
- [7] J. Manning, R. Olshansky and C.B. Su, "The carrier-induced index change in AlGaAs and 1.3 μm InGaAsP diode lasers," *IEEE J. Quantum Electron.*, vol. QE-19, October 1983.
- [8] J.K. Butler, D.E. Ackley and D. Botez,

- Coupled Modes in Phase-Locked Injection Laser Arrays*. Seventh Topical Meeting on Optical Fiber Communications, New Orleans, Louisiana, January 23-25, 1984.
- [9] J.K. Butler, D.E. Ackley and D. Botez, "Coupled-mode analysis of phase-locked injection laser array," *Appl. Phys. Lett.*, vol. 44, pp. 293-295, Feb. 1984.
- [10] E. Kapon, J. Katz and A. Yariv, "Super-mode analysis of phase-locked arrays of semiconductor lasers," *Opt. Lett.*, vol. 10, pp. 125-127, April 1984.
- [11] S.R. Chinn and R.J. Spiers, "Modal gain in coupled-stripe lasers," *IEEE J. Quantum Electron.*, vol. QE-20, pp. 358-363, April 1984.
- [12] J.K. Butler, D.E. Ackley and M. Ettenberg, "Coupled-mode analysis of gain and wavelength oscillation characteristics of diode laser phased arrays," *IEEE J. Quantum Electron.*, vol. QE-21, pp. 458-464, May 1985.
- [13] E.A.J. Marcatili, "Dielectric rectangular waveguide and directional coupler for integrated optics," *Bell Sys. Tech. J.*, vol. 48, pp. 2071-2102, Sept. 1969.
- [14] D. Marcuse, *Light Transmission Optics*, Van Nostrand Reinhold Co., New York, N.Y., 1972.
- [15] D. Botez, "Array-mode far-field patterns for phase-locked diode-laser arrays: coupled-mode theory versus simple diffraction theory," *J. Quantum Electron.*, vol. QE-21, pp. 1752-1755, Nov. 1985.
- [16] D. Botez and D.E. Ackley, "Phase-locked Arrays of Semiconductor Diode Lasers," *IEEE Circuit and Dev. Mag.*, pp. 8-17, Jan. 1986.
-